

# An experimental study of non-Newtonian fluid flow in rectangular flumes in laminar, transition and turbulent flow regimes

R Haldenwang, P T Slatter and R P Chhabra

New and extensive results are reported on the flow of a range of non-Newtonian fluids, including aqueous suspensions of bentonite and kaolin, and aqueous solutions of synthetic polymer carboxymethyl cellulose (CMC), flowing down inclined flumes of rectangular cross-section of three different sizes. In particular, these tests elucidate the role of shear-thinning viscosity, with and without the presence of a yield stress, on the flow behaviour in flumes over a wide range of conditions of Reynolds numbers spanning the range  $1 < Re < 10^4$ , thereby embracing both the laminar and transitional flow regimes, and possibly the turbulent regimes. Furthermore, the flumes could be tilted up to  $5^\circ$  from the horizontal. This extensive experimental study has facilitated the delineation of the role of the Froude number in the nature of flow, as well as the cessation of laminar flow conditions in such industrially important systems. The results reported here can be used to design flumes for shear-thinning and/or viscoplastic fluids.

## INTRODUCTION

Reliable methods for the analysis and design of open channels that transport water and other Newtonian fluids have been developed over the past 120 years, and are available in standard textbooks (e.g. Chow 1959; Chadwick & Morfett 1999; Chanson 1999; Douglas et al 1985). Owing to the low viscosity of such fluids, the flow conditions almost inevitably relate to the turbulent flow regime for water and raw sewage. Remarkably, the approach developed by Manning in 1890 is accurate and is still widely used for analysing the performance of an existing channel and for designing a new installation (Manning 1890). On the other hand, it is readily acknowledged that many materials – notably particulate suspensions – encountered in mineral processing, mud flows, spreading of lava and tailings disposal applications exhibit complex flow behaviour which cannot be described even qualitatively by the Newtonian fluid postulate. For instance, almost all suspensions display the so-called “shear-thinning phenomenon”, wherein their effective (apparent) viscosity, defined as shear stress divided by shear rate, decreases with increasing shear rate. Indeed, the viscosity of a shear-thinning fluid can decrease by several orders of magnitude under appropriate conditions (Chhabra & Richardson 2008). Furthermore, some of the industrial fluids also exhibit a yield stress – a threshold

value below which the material behaves like an elastic solid. Once the applied shear stress exceeds the yield stress, the substance behaves like a fluid, with or without the occurrence of shear-thinning behaviour.

Admittedly, some materials also exhibit time-dependent and/or visco-elastic behaviour, but it seems reasonable to begin with the simplest type of non-Newtonian fluid behaviour, namely pseudoplastic (shear thinning without yield stress) and yield pseudoplastic (shear thinning with yield stress). Thereafter the level of complexity can be gradually built up to accommodate the other features, such as visco-elasticity and time-dependence. Therefore, this work is concerned with the flow of pseudoplastic and yield-pseudoplastic fluids in rectangular flumes.

In addition to the use of flumes and launders, similar free surface flows of such fluids are also encountered in nature, such as debris flows (landslides) and spreading of lava, but several industrial applications also entail the free surface flow of such non-Newtonian systems, e.g. in food processing, painting, sewage sludge, etc. In spite of their frequent occurrence in numerous industrial settings, very little, especially experimental, work has been reported on the flow behaviour of time-independent non-Newtonian fluids in open channels and flumes. A concise survey of the previous pertinent literature follows.

## TECHNICAL PAPER

### JOURNAL OF THE SOUTH AFRICAN INSTITUTE OF CIVIL ENGINEERING

Vol 52 No 1, 2010, Pages 11–19, Paper 682



PROF RAINER HALDENWANG received his NHD, MDipl & DTech (civil engineering) from the Cape Peninsula University of Technology. After graduating, he spent 10 years in harbour engineering at Saldanha Bay working for Portnet. In 1978 he joined the then Cape Technikon as a lecturer in civil engineering. He is currently Associate Professor in the Department of Civil

Engineering and Surveying, responsible for the final-year research projects and lecturing in fluid mechanics. He also heads a research group investigating the flow behaviour of non-Newtonian fluids in pipes, flumes, fittings and pumps.

#### Contact details

Department of Civil Engineering and Surveying  
Cape Peninsula University of Technology  
PO Box 652  
Cape Town 8000  
T: 021 460 3512  
F: 021 460 3990  
E: haldenwang@cput.ac.za



PROF PAUL SLATTER, BSc (Eng) (Natal), MSc (Eng) and PhD (UCT), is Professor of Rheology and Fluid Engineering at RMIT University, Melbourne, Australia. He has been teaching and researching the flow behaviour of non-Newtonian materials since 1983. After developing novel methods for rheological characterisation from tube flow, he developed transitional and turbulent pipe flow

models based on dynamic similarity. These approaches are being extended to the analysis of sheet flow, open channel flow, fittings losses and pump derating. Paul is a Fellow of SAICE, the Water Institute of Southern Africa and the Southern African Institute of Mining and Metallurgy.

#### Contact details

School of Civil, Environmental and Chemical Engineering  
RMIT University  
24 La Trobe St  
Melbourne, Victoria, 3000  
Australia  
E: paul.slatter@rmit.edu.au



DR RAJ P CHHABRA received his BS, MS and PhD (chemical engineering) from the University of Roorkee (India), the Indian Institute of Science, Bangalore, and Monash University (Australia), respectively. After post-doctoral work at the University College of Swansea (UK), he became an Assistant Professor and later Professor of Chemical Engineering at the Indian Institute of Technology.

His main research interests are in the field of non-Newtonian multi-phase flows. He has lectured extensively in the US, Canada, Europe, the UK, Australia, Japan and South Africa and is a Fellow of the Indian National Academy of Engineering.

#### Contact details

Department of Chemical Engineering  
Indian Institute of Technology  
Kanpur, India  
T: 91 512 259 7393  
F: 91 512 259 0104 / 259 0007  
E: chhabra@iitk.ac.in

Keywords: open channel, flume, non-Newtonian fluids, Froude number, friction factor

**Table 1 Test fluid characteristics**

Fluid	$\rho$ (kg/m <sup>3</sup> )	$\tau_y$ (Pa)	$K$ (Pa.s <sup>n</sup> )	n
3,0% kaolin suspension	1 050	1,73	0,004	0,955
4,5% kaolin suspension	1 075	3,51	0,012	0,836
5,3% kaolin suspension	1 088	4,99	0,030	0,717
6,0% kaolin suspension	1 099	6,84	0,148	0,517
8,0% kaolin suspension	1 118	9,34	0,208	0,539
9,0% kaolin suspension	1 149	20,40	0,267	0,535
10,0% kaolin suspension	1 165	21,30	0,524	0,468
3,0% bentonite suspension	1 014	1,00	0,003	1
4,5% bentonite suspension	1 025	4,40	0,006	1
6,0% bentonite suspension	1 033	12,70	0,006	1
1,0% CMC solution	1 007	–	0,060	0,655
1,5% CMC solution	1 009	–	0,018	0,947
1,8% CMC solution	1 011	–	0,087	0,765
2,8% CMC solution	1 016	–	0,197	0,758
3,8% CMC solution	1 021	–	0,606	0,678

Currently available, limited literature in the field can be conveniently divided into three categories based on the motivation. Owing to the simplicity of the flow geometry, early studies were aimed at evaluating the rheological constants for a range of materials by postulating the laminar flow to be one-dimensional, steady and uniform on an inclined surface. Under these conditions, the shear stress varies linearly from a maximum value at the wall to zero at the free surface. Thus, one can parallel the analysis of Rabinowitsch-Mooney for the flow in tubes to derive an expression for the shear rate at the wall from the flow depth–inclination data, as outlined by Chhabra and Richardson (2008). The early work done by Astarita et al (1964) and Paslay and Slibar (1958) demonstrates the utility of this approach for power law and Bingham plastic model fluids. Subsequently, this approach received further support from the experimental results reported by Therien et al (1970) and Sylvester et al (1973). Later this method was also shown to be applicable not only to the other non-Newtonian viscosity models (De Kee et al 1990; Coussot 1994, 1997), but also to the determination of the yield stress without invoking a fluid model *a priori* (Uhlherr et al 1984). In essence, the above studies treat this flow as viscometric and allude to the possibility of using the method as a viscometer, although many unresolved issues, such as the end-effects, the role of surface tension, etc, continue to be some of the main impediments in this direction.

The second category of studies has been motivated by engineering applications, such

as estimating the drainage of thin films adhering to the walls of vessels in engineering applications. These studies attempt to develop frameworks for the prediction of flow rate for a presupposed fluid model and a flume of known geometry. Of course, these two categories of study are not mutually exclusive. For instance, Kozicki and Tiu (1967) were seemingly the first to develop a general framework for the laminar flow of time-independent non-Newtonian fluids in ducts of non-circular cross-section. Their approach leads to the usual friction factor–Reynolds number relationship. This method hinges on the identification of two geometric parameters which are fixed for a given shape, and are assumed to be independent of fluid behaviour. This approach has been tested extensively for the flow of inelastic non-Newtonian fluids in ducts of square, rectangular and triangular cross-sections over wide ranges of conditions, but not for the flow in open channels, except for the recent work by Haldenwang et al (2002) and Haldenwang (2003). Naik (1983) reported extensive results on the flow of kaolin and sand slurries. However, not only did most of his data relate to turbulent flow conditions in open channels, but he did not perform adequate rheological characterisation of his test fluids. Therefore, it is not at all possible to delineate the role of non-Newtonian characteristics from his study. Wilson (1991) used heuristic arguments to extend to power law fluids the approach used for the design of flumes to transport Newtonian fluids. In an attempt to gain physical insights, Sanders et al (2002) measured velocity profiles in open channels

for coarse particles being transported in non-Newtonian slurries.

All these studies are based on the assumption of uniform steady and one-dimensional flow. The third category consists of the studies in which one or more of these assumptions was relaxed. For instance, non-uniform and steady flows in long vessels were studied by Wilson and Taylor (1996) and Taylor and Wilson (1997). Similarly, unsteady flows as encountered in the spreading of lava, or the spreading of a yield stress material during the slump test, were investigated within the framework of slow flow by Huang and Garcia (1998), Balmforth et al (2000), etc. The effect of finite channel width has been investigated by Mei and Yuhi (2001). Excellent survey articles summarising these and other studies are available in the literature (Balmforth et al 2007).

From the above discussion it is clear that significant theoretical advances have been made in the field of non-Newtonian fluids on inclined surfaces. However, only very limited experimental results are available on the friction factor–Reynolds number relationship for the flow of such fluids in open channels, although this relationship is of considerable importance for both theoretical and pragmatic reasons in numerous settings. Nor has there been a systematic study on delineating the end of laminar flow conditions and the onset of the turbulent flow regime for the flow of non-Newtonian fluids in flumes. This work endeavours to fill these gaps in the current knowledge on this subject.

## EXPERIMENTAL MATERIALS AND PROCEDURE

The test fluids used in this study consisted of aqueous suspensions of bentonite and kaolin clays, and aqueous solutions of carboxymethyl cellulose polymer of various concentrations. The fluids were prepared by gradually adding the requisite amount of dry solids to the measured quantity of water, followed by gentle agitation. Over the concentration range and flow conditions used here, there was no detectable settling of the suspensions; the polymer solutions are known to be stable over a long period of time. All materials tested were thus treated as homogeneous continua. The shear stress–shear rate behaviour of each test fluid was measured using pipeline viscometers as described in the next section. Their densities were measured using a constant-volume density bottle. The physical characteristics of the test fluids are summarised in Table 1. In all, 14 test fluids were employed to encompass wide ranges of rheological characteristics and of the Reynolds number.

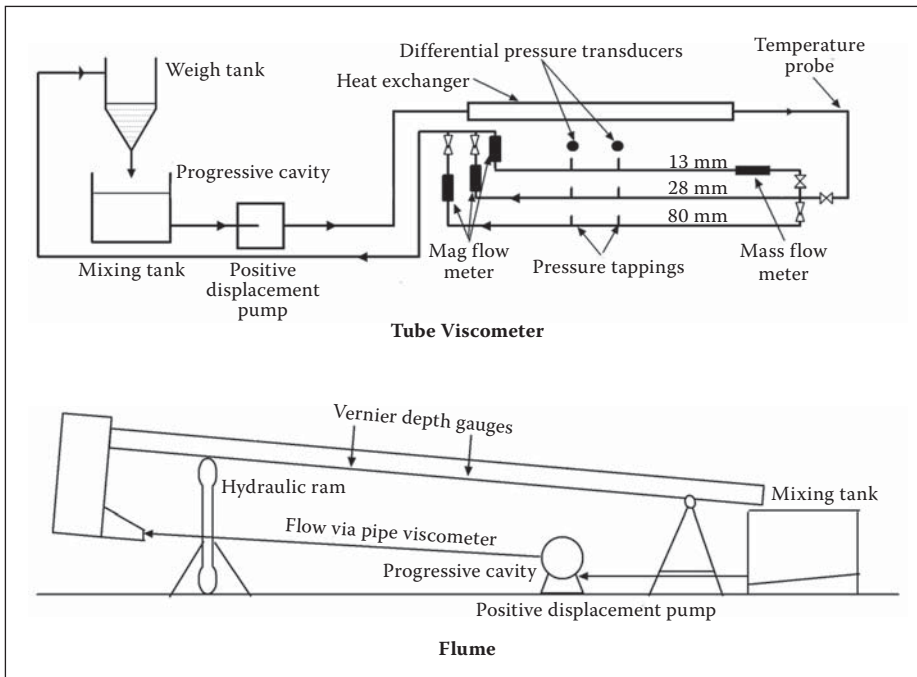


Figure 1 Flume and tube viscometer

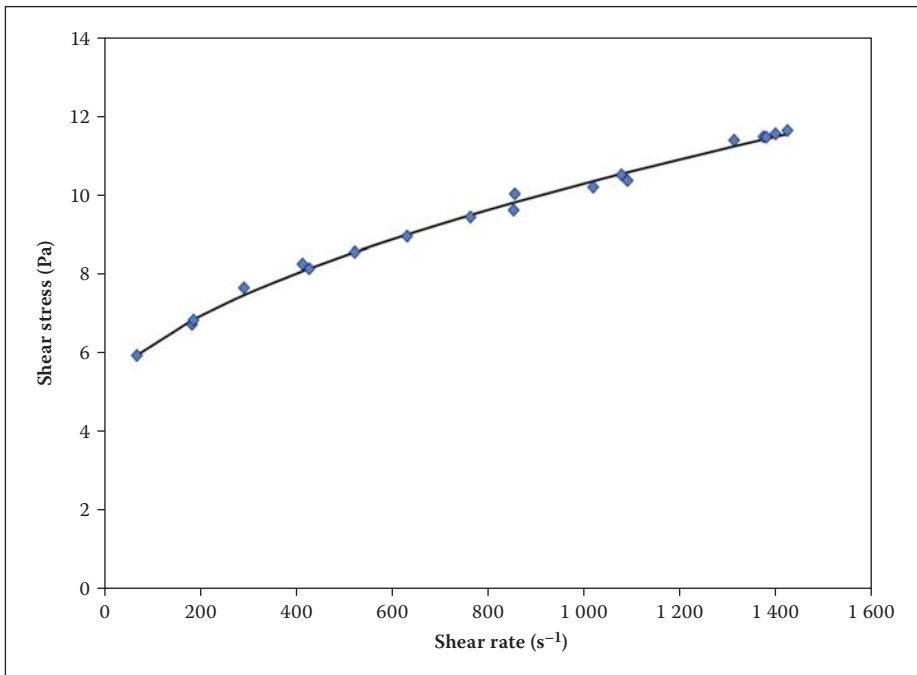


Figure 2 Flow curve for 6% kaolin suspension

The flume tests were conducted in two tilting flumes, one 10 m long by 300 mm wide, and the other 5 m long by 75 mm wide, both of which can be tilted up to 5° from the horizontal. The 300 mm-wide flume can be longitudinally partitioned to a width of 150 mm. The flow was provided by a 100 mm progressive cavity, positive-displacement pump or a Warman 4 x 3 centrifugal slurry pump, depending on the desired flow rate. The maximum flow rate achieved in this study was 45 litres per second.

Flow depths were measured with digital depth gauges fitted at distances of 5 and 6 m downstream of the inlet of the 10 m flume. These distances were found to be adequate

to ensure that the entrance and exit effects would be negligible (Haldenwang 2003). The difference between the values of the fluid depth between these two locations was found to be ±5% and therefore the flow depth was assumed to be uniform.

The flume tests consisted of measuring the flow rate with magnetic flow meters and the flow depth with digital depth gauges, for various channel slopes from 1° to 5°. All the instruments were linked to a PC via a data-logger. The calibrated data inputs were recorded and computationally reduced to values of Reynolds number and friction factor, and then plotted as a Moody diagram. This enabled deviations to be observed instantaneously. For each

size flume, sets of flow data were collected for various concentrations, slopes and flow rates, as well as tube viscometer data for each concentration.

The flumes were connected by means of pipes to an in-line tube viscometer (with three tubes of different diameters, namely 13, 28 and 80 mm), as shown schematically in Figure 1.

Each tube was fitted with a magnetic flow meter and differential pressure transducers to measure the pressure drop across a fixed straight length of the pipe. From these measurements, the nominal shear rate ( $8V/D$ ) and the average wall shear stress data can be calculated (Chhabra & Richardson 2008). The estimated uncertainty in wall shear stress is less than 5% and that in the nominal shear rate less than 0,5% (Haldenwang 2003). These data were then used to evaluate the true shear stress–shear rate behaviour of the test fluids used in this study.

## TREATMENT OF EXPERIMENTAL DATA

### Rheological behaviour of test fluids

Using the pressure drop–flow rate data obtained from the three pipe loops, it is customary to calculate the wall shear stress–nominal shear rate at the pipe wall as follows:

$$\tau_w = \frac{D}{4} \left( -\frac{\Delta p}{L} \right) \quad (1)$$

$$\dot{\gamma}_{wn} = \frac{8V}{D} \quad (2)$$

The true shear rate at the wall is given by applying the Rabinowitsch-Mooney correction factor to the nominal shear rate given by Eq (2) as follows (see Chhabra & Richardson 2008 for details):

$$\dot{\gamma}_w = \left( \frac{3n' + 1}{4n'} \right) \left( \frac{8V}{D} \right) = \left( \frac{3n' + 1}{4n'} \right) \dot{\gamma}_{wn} \quad (3)$$

where

$$n' = \frac{d \ln \tau_w}{d \ln \left( \frac{8V}{D} \right)}$$

which is evaluated at the pertinent value of the nominal wall shear stress. Figure 2 shows typical shear stress–shear rate behaviour for a 6% kaolin suspension. The fact that the results for the different pipe diameters collapse onto a single curve is evidence that these data are free from slip and end-effects (Chhabra & Richardson 2008). Similar results were obtained for the other test fluids used in this work, but for the sake of brevity they are not included here.

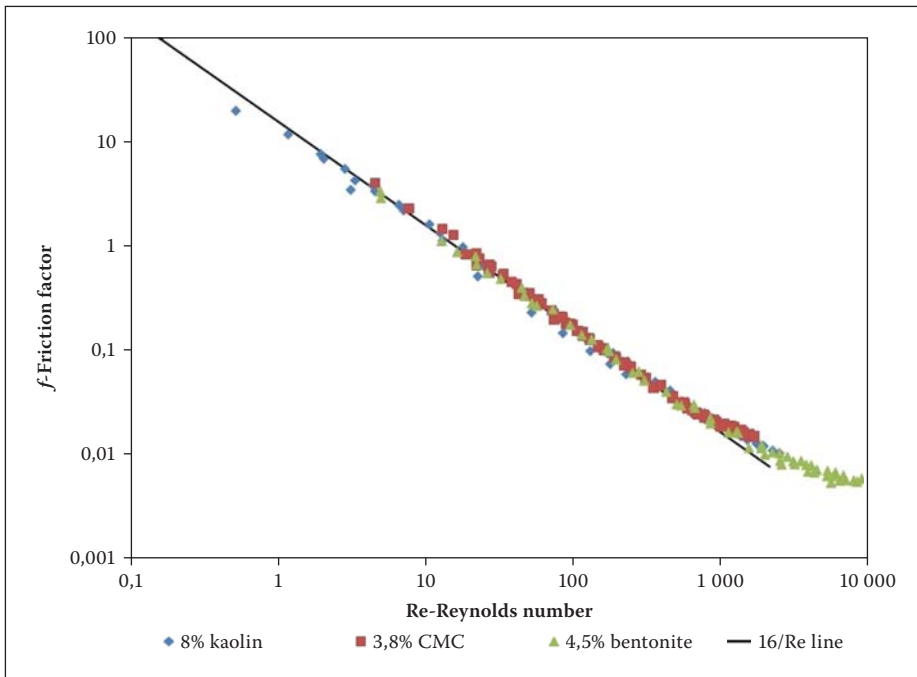


**Figure 3** Typical Moody diagram for 300 mm flume with 3 different fluids

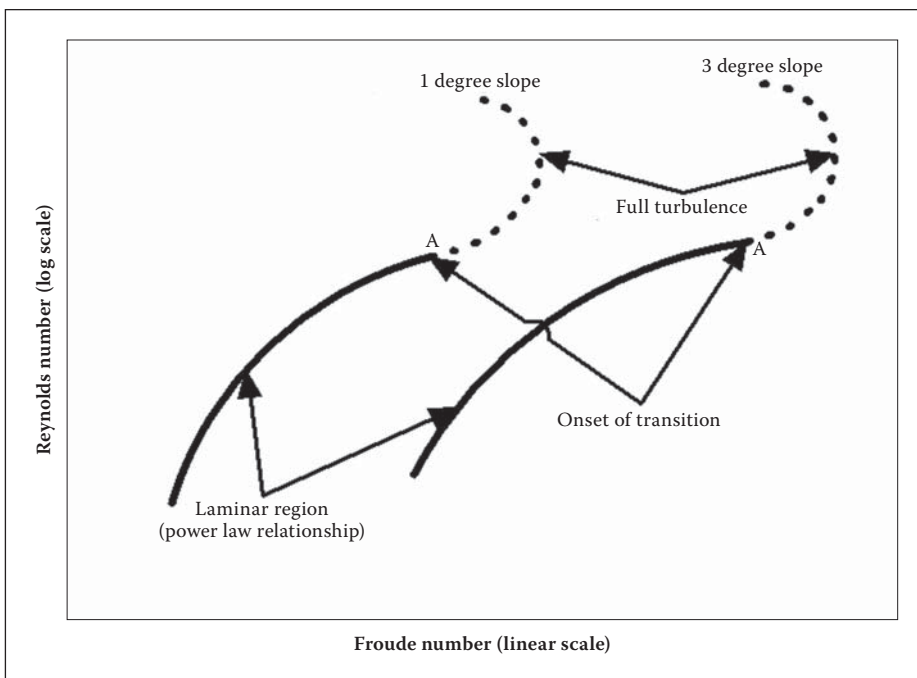


**Figure 4** Reynolds number against Froude number (typical experimental behaviour)

Once the true shear stress–shear rate data are available, it is customary to fit a rheological model to these. In view of the fact that all the test fluids used in this work displayed shear-thinning behaviour, and that the kaolin and bentonite suspensions also displayed the presence of a yield stress, the Herschel-Bulkley rheological model was used here which, in simple shear, is written as:

$$\tau = \tau_y + K\dot{\gamma}^n \quad (4)$$

Eq (4) includes the Newtonian ( $n = 1$ ;  $\tau_y = 0$ ), Bingham plastic ( $n = 1$ ) and power-law ( $\tau_y = 0$ ) fluid models as limiting cases, and it is thus extremely versatile in capturing a range of non-Newtonian characteristics.

The best-fit values of  $\tau_y$ ,  $K$  and  $n$  were found by performing non-linear regression on the shear stress–shear rate data for each fluid. The error analysis performed indicated that the accuracies of  $\tau_y$ ,  $K$  and  $n$  were in the region of 2, 7 and 3% respectively. The resulting values of these constants are also summarised in Table 1.

#### Flume data (flow rate-inclination)

It is also customary to convert the flow rate–inclination data for a given fluid into dimensionless form. When ( $H/w$ ) < 0,1, it is perhaps reasonable to postulate that the flow is one-dimensional and the end-effects are negligible. Under these conditions the shear stress at the wall is given by:

$$\tau_w = \rho g H \sin \theta \quad (5)$$

where  $H$  is the uniform flow depth.

As the  $H/w$  values in laminar flow were in many instances > 0,1, the hydraulic diameter was used, with the average wall shear stress for the open channel being given as (Sanders et al 2002):

$$\tau_w = \rho g D_h \sin \theta \quad (6)$$

A convenient non-dimensional shear stress is written in terms of the Fanning friction factor ( $f$ ) as follows:

$$f = \frac{\tau_w}{\left(\frac{1}{2}\right)V^2\rho} \quad (7)$$

The other pertinent dimensionless parameter is, of course, the Reynolds number,  $Re$ . For Newtonian fluids, one can define the Reynolds number in an unambiguous manner as:

$$Re = \frac{\rho V L_c}{\mu} \quad (8)$$

where the characteristic linear dimension  $L_c$  is usually taken as the hydraulic diameter  $D_h$  for non-circular cross-sections. For  $H/w \ll 1$ ,  $D_h = 4H$  (Chow 1959; Chanson 1999).

On the other hand, the choice of a suitable definition of the Reynolds number for non-Newtonian fluids is far from clear, although several plausible definitions (Chhabra & Richardson 2008) are given in the literature. However, here we use the definition introduced by Slatter and Lazarus (1993), which has also proved to be of value in reconciling much of the literature data on turbulent flow of non-Newtonian fluids in pipes (Slatter 1999). By substituting  $D = D_h$ , it is written here as:

$$Re = \frac{8\rho V^2}{\tau_y + K\left(\frac{8V}{D_h}\right)^n} \quad (9)$$

It is useful to emphasise here that within the limits of Newtonian fluid behaviour, (i.e.  $\tau_y = 0$ ;  $n = 1$ ), Eq (9) reduces to the familiar definition of the Reynolds number for Newtonian fluids. For this reason each experimental data point was reduced to an  $f$ - $Re$  coordinate. It should be recalled that the friction factor and Reynolds number defined above not only reconcile the data with  $f = 16/Re$  in laminar flow conditions, but also permit the use of the standard Moody diagram for Newtonian fluids (Chow 1959), even in the turbulent flow regime. Dimensional considerations also suggest that the flow in open channels is influenced by the value of the Froude number,  $Fr$ , which is defined as:

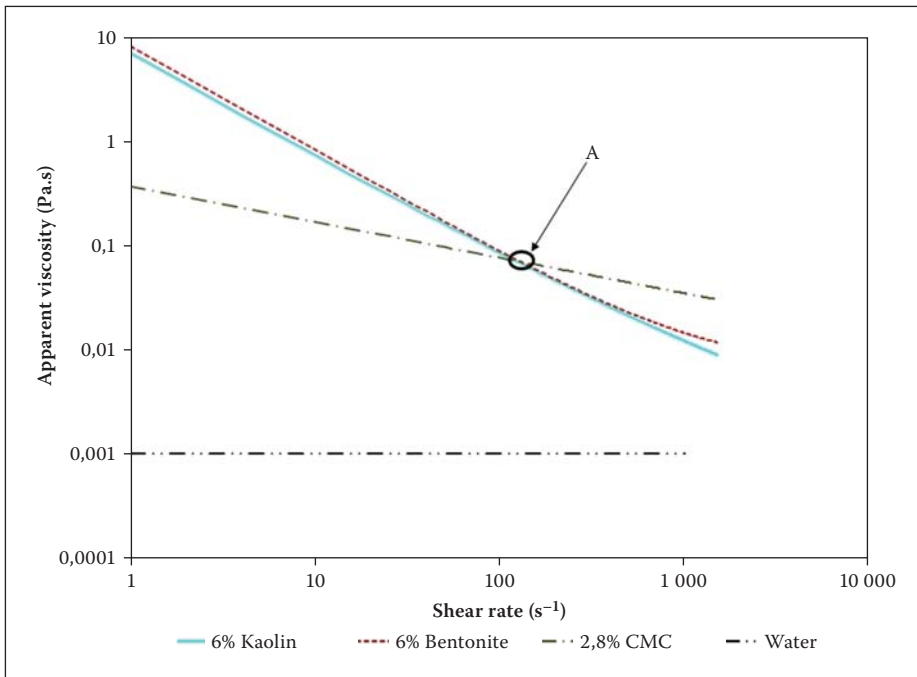


**Figure 5** Apparent viscosity against shear rate for 6% kaolin, 6% bentonite and 2,8% CMC and water

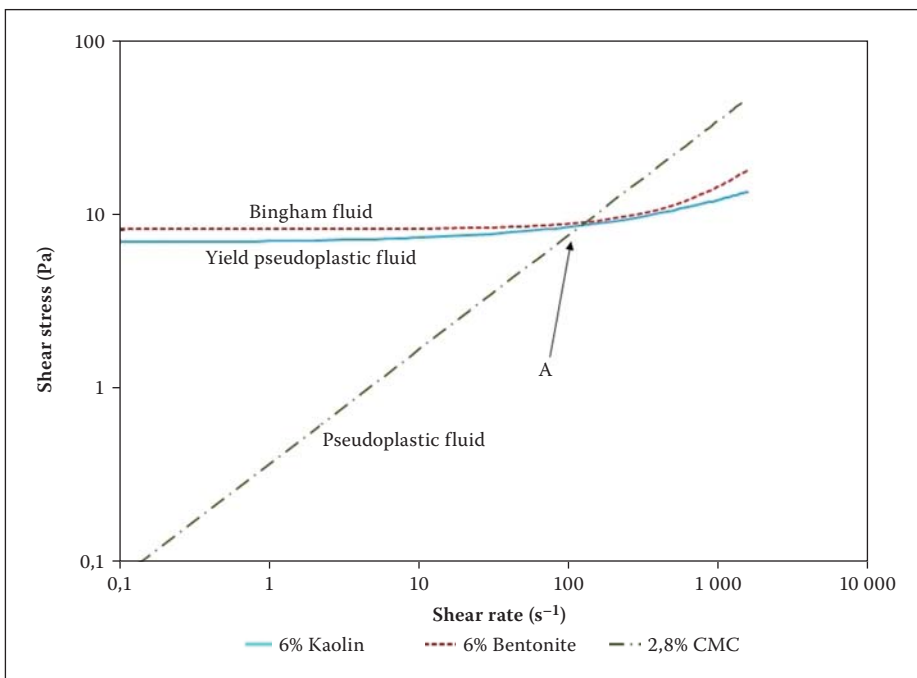


**Figure 6** Rheogram for 6% kaolin, 6% bentonite and 2,8% CMC

$$Fr = \frac{V}{\sqrt{gH}} \quad (10)$$

Depending on the value of the Froude number, the flow is classed as sub-critical ( $Fr < 1$ ) or super-critical ( $Fr > 1$ ); the former is dominated by gravity while the inertial forces dominate the latter. The flow is said to be critical at  $Fr = 1$ .

Thus, in summary, the flow of non-Newtonian fluids in an open channel can be described in terms of the three dimensionless parameters:  $f$ ,  $Re$ , and  $Fr$ . This relationship is explored in the next section.

It should be borne in mind that for the flow of Newtonian fluids in circular pipes, the use of the  $f$ - $Re$  coordinates leads to the well-known Moody diagram which shows

a distinct signature corresponding to the cessation of laminar flow conditions at  $Re = 2\,100$ , i.e. the values of the friction factor begin to deviate from the expected laminar flow characteristics given by:

$$f = \frac{16}{Re} \quad (11)$$

Although the laminar flow conditions cease to exist at  $Re \sim 2\,100$ , the fully turbulent regime is preceded by a transition zone. Needless to say, the friction factors in the transition and turbulent regions have been correlated empirically by numerous equations of varying forms and complexity. Beyond the laminar flow regime, the value of the friction factor is also influenced by the pipe

wall roughness. This approach has also been extended to power law and visco-plastic fluids in circular tubes and pipes, albeit not as successfully as with the Moody diagram (Govier & Aziz 1977). In view of the simplicity of this approach, it is natural to explore the possibility of extending it to flow in open channels, as demonstrated in the next section.

## RESULTS AND DISCUSSION

At the outset, the results were plotted using  $f$ - $Re$  (given by Eq (9)) coordinates. Figure 3 shows a representative sample of the friction factor-Reynolds number relationship for three different fluids in the 300 mm-wide flume. Similar results were obtained for the other fluids and/or flume inclinations, but are not included here to avoid cluttering the figures due to the numerous overlapping data points. Clearly, the definition of the Reynolds number given by Eq (9) **does** confirm the validity of Eq (11) for the flow of time-independent non-Newtonian fluids in open channels as well.

Though there is considerable confusion in the literature regarding the turbulent flow of non-Newtonian fluids even in pipes, Slatter (1996) developed the following semi-empirical form of the velocity profile in a pipe under turbulent conditions.

$$\frac{V}{V_*} = \frac{1}{\lambda} \ln \left( \frac{R}{d_{85}} \right) + B - 3,75 \quad (12)$$

This will also be used here to analyse the present results for open channel flow. However, what is less obvious in this approach is the critical value of the Reynolds number denoting the limit of laminar flow conditions, akin to that observed in circular pipes.

Intuitively, one would expect the role of the Froude number to be much more significant here than that in the laminar flow regime.

The plots of Reynolds number against Froude number revealed a characteristic shape, which distinctly indicated a change of gradient effect corresponding to the end of the laminar flow regime, as shown in Figure 4.

The onset of fully turbulent conditions manifested in terms of another distinct change in shape of the  $Re$ - $Fr$  map. This form of behaviour was observed for all data sets.

Evidently, what would be of great practical utility is to link these transition points (seen as a change of gradients and shown as inflection points A on Figure 4) to the measurable rheological properties of the test fluids. This link was established in an empirical manner by examining the apparent viscosity values at a range of shear rates (50, 100, 200 and 500  $s^{-1}$ ). It is worthwhile to emphasise

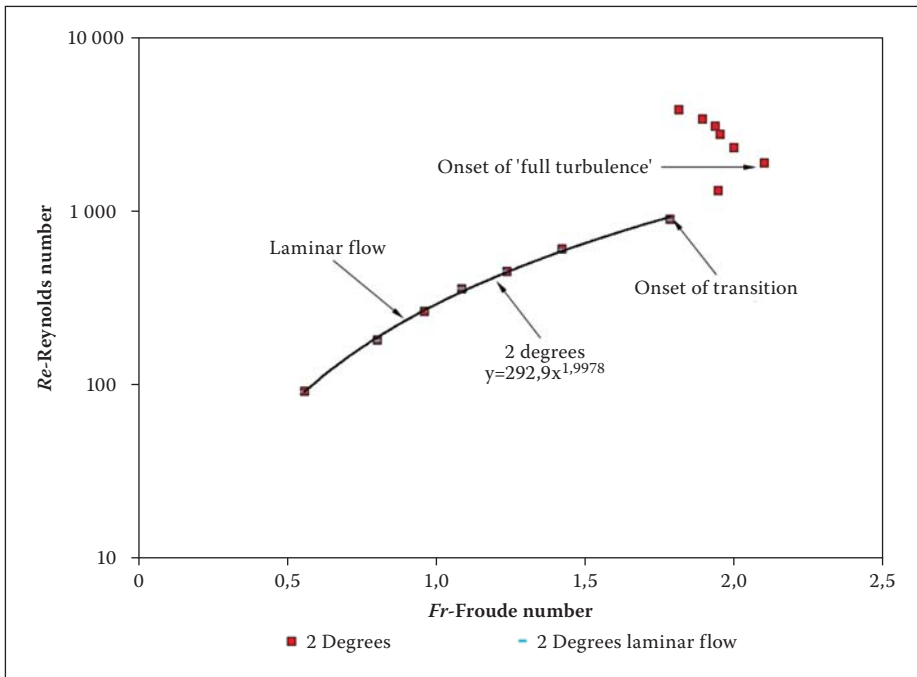


Figure 7 Empirical behaviour of 2,8% CMC in 150 mm flume

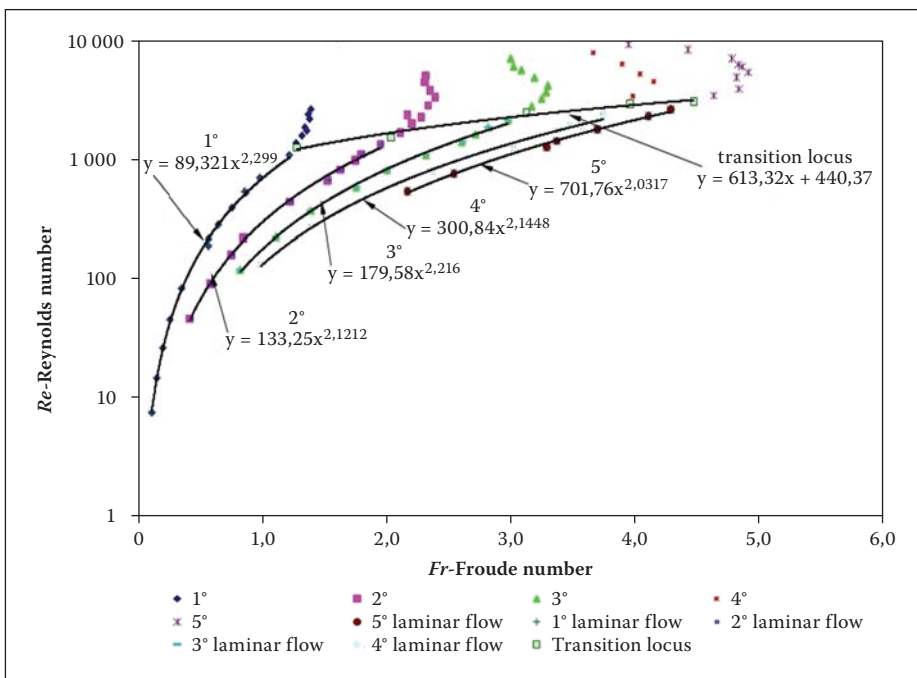


Figure 8 Onset of transition locus for 4,6% bentonite in 150 mm flume

here that the viscous effects are only of secondary importance in the turbulent flow regime (Slatter 1999).

Figure 5 shows apparent viscosity against shear rate for 6% bentonite, 6% kaolin and 2,8% polymer carboxymethyl cellulose (CMC) and it can be clearly observed that the apparent viscosity of these fluids is very similar at a shear rate of  $100 \text{ s}^{-1}$ . One would expect the corresponding values of shear stress to be similar, as seen in Figure 6. Detailed analysis of the experimental data revealed that  $\dot{\gamma}=100 \text{ s}^{-1}$  is probably a representative shear rate of the transition point, although it is difficult to offer any theoretical justification for this assertion and it is entirely an empirical observation.

The next step was to establish a relationship between the apparent viscosities of a specific slurry and the Froude number as observed from the plot of Reynolds number and Froude number for each slope. Based on the flow behaviour, the start of transition was deemed to be the point of inflection, as this point corresponds in all cases to the deviation from the  $16/Re$  line on the Moody diagram. This is shown in Figure 7 which portrays typical behaviour. Furthermore, the onset of full turbulence was held to occur at a point where the Froude number attains the maximum value of these plots in each case. The transition regime therefore occupies the region between these two points.

### Onset of transition

The points of inflection were connected and the linear relationship was established between these points to establish a transition locus for a given fluid, as shown in Figure 8. This was done for all the data sets. Thereafter the gradient and ordinate-intercept for each relationship was plotted against the apparent viscosities at shear rates of 50, 100 and  $200 \text{ s}^{-1}$ .

These shear rates were chosen on the basis of a detailed analysis of the experimental data as it was reasoned that the onset of transition would usually occur in the lower shear rate region. The apparent viscosity at a shear rate of  $100 \text{ s}^{-1}$  yielded the best results.

From this a trend was established between the gradient (M) and the ordinate-intercept (C) values, with the apparent viscosities at the shear rate of  $100 \text{ s}^{-1}$ .

The relationship between M and the apparent viscosity at  $100 \text{ s}^{-1}$  is best approximated as follows:

$$M = 853,1 \left( \frac{\mu_{\dot{\gamma}=100 \text{ s}^{-1}}}{\mu_w} \right)^{-0,21} \quad (13)$$

The relationship between C and the apparent viscosity at  $100 \text{ s}^{-1}$  is as follows:

$$C = 1,263 \times 10^4 \left( \frac{\mu_{\dot{\gamma}=100 \text{ s}^{-1}}}{\mu_w} \right)^{-0,75} \quad (14)$$

The value of the critical Reynolds number at the onset of transition is:

$$Re_c = 853,1 \left( \frac{\mu_{\dot{\gamma}=100 \text{ s}^{-1}}}{\mu_w} \right)^{-0,21} Fr + 1,263 \times 10^4 \left( \frac{\mu_{\dot{\gamma}=100 \text{ s}^{-1}}}{\mu_w} \right)^{-0,75} \quad (15)$$

where  $\mu_w$  is the viscosity of water taken as  $10^{-3} \text{ Pa.s}$ .

The critical Reynolds number does not have a single value, but is a relationship between Reynolds number and Froude number for the specific apparent viscosity. The position of the onset of transition is given by the intersection point of the equation (Eq 15) and the laminar flow equation, i.e.  $f = 16/Re$ . This is an iterative process to obtain the value of the flow such that both these equations are satisfied simultaneously.

### Onset of turbulence

The approach used above to locate the end of the laminar flow regime was paralleled to delineate the onset of turbulent conditions, reflected as another change in gradient in the Re-Fr plot, as shown in Figure 9. This corresponds to the maximum value of the Froude number. The points where the Froude number was at a maximum were connected and a linear relationship was determined.

From this a trend was established between the M and C values, and the apparent viscosity.

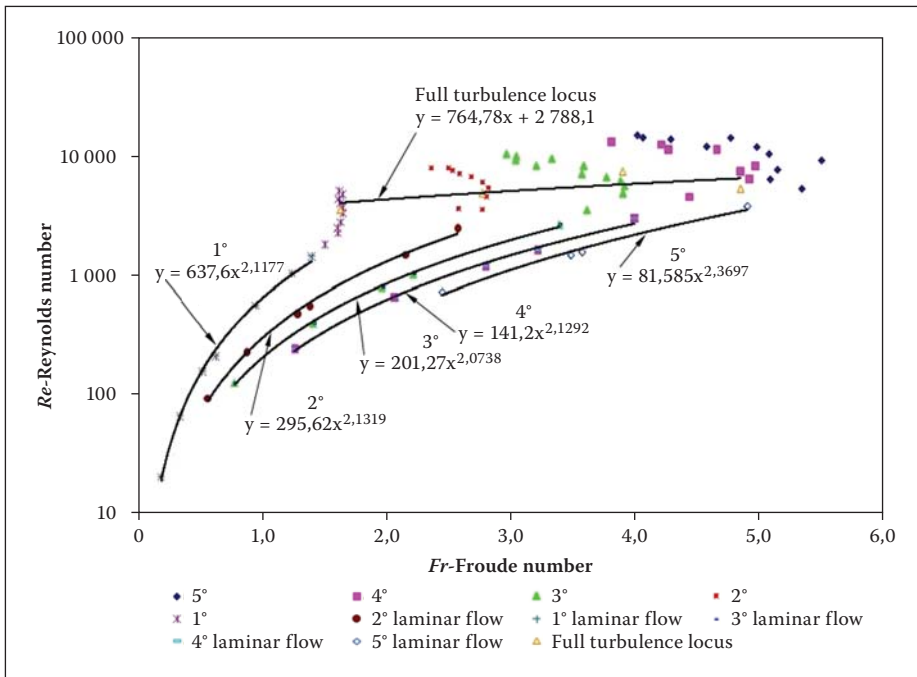


Figure 9 Onset of "full turbulence" 4,5% kaolin in 150 mm flume

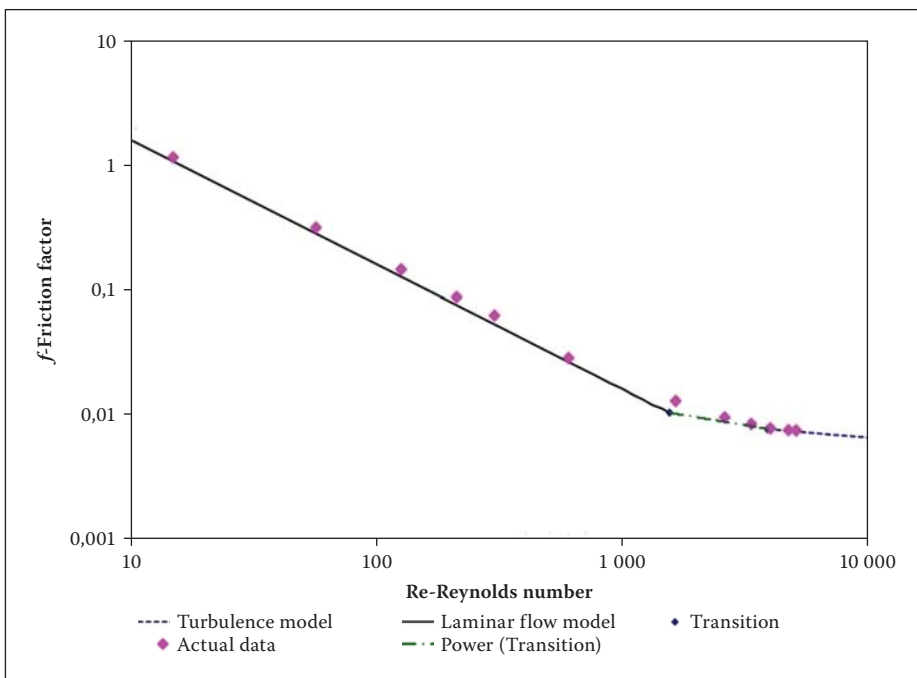


Figure 10 Moody diagram of 6% bentonite in 150 mm flume with 4° slope

The best relationship was for the apparent viscosity at a shear rate of  $500 \text{ s}^{-1}$ .

The value of the critical Reynolds number at the onset of "full turbulence" or the end of transition is:

$$Re_{c(turb)} = \frac{3812}{\left(\frac{\mu/\dot{\gamma}=500\text{s}^{-1}}{\mu_w}\right)^{0,52}} Fr + \frac{9626}{\left(\frac{\mu/\dot{\gamma}=500\text{s}^{-1}}{\mu_w}\right)^{0,65}} \quad (16)$$

This critical Reynolds number again does not have a single value, but is a relationship between Reynolds number and Froude number for the specific apparent viscosity. The position of the onset of transition is where the  $Re_{c(turb)}$  (Eq 16) intersects with the turbulent flow equation (Eq 12), slightly

modified by incorporating the apparent viscosity at a shear rate of  $500 \text{ s}^{-1}$  to be consistent with the above phenomenological considerations (Haldenwang 2003). This leads to the following expression for average velocity:

$$V_{turb} = \sqrt{gH\sin\alpha} \left( 2,5\ln \frac{2R_h}{k} - 76860 \left( \frac{\mu/\dot{\gamma}=100\text{s}^{-1}}{\mu_w} \right) - 9,45 \right) \quad (17)$$

Thus the critical Reynolds number denoting the onset of turbulent flow is obtained by simultaneously solving Eq (16) and Eq (17).

Lastly, based on the above analysis together with the detailed inspection of the extensive database, it is worth reiterating the following overall trends:

- In laminar flow conditions, the present extensive data for a range of fluids conform to the expected behaviour, namely,  $f = 16/Re$ .
- At low concentrations (< 3% for bentonite, < 5% for kaolin and < 2% for CMC), a sudden increase in the value of the friction factor in the transition regime of  $Re = 2\,000$  to  $8\,000$  was observed – similar to that of water – a sudden jump in a very unstable region. This sudden increase was very difficult to measure and characterise due to the inherently fluctuating and unstable nature of the flow under these conditions. With increasing flow rate, the free surface became increasingly irregular, and a point was reached where the flow height was measured on top of the irregularities which manifested as the sudden increase in friction factor to full turbulence. The more viscous the fluid, the smoother the transition region, and the lower was the critical Reynolds number where the data began to deviate from the laminar  $16/Re$  line.
- It appears from experimental evidence that the critical Reynolds number cannot be fixed to a classically narrow region as in the case of a pipe, but occurs over a much wider range of Reynolds numbers, depending on the viscous characteristics of the fluid.
- This trend was consistent for three very different rheologically classified fluids, namely bentonite, kaolin and CMC.

## ILLUSTRATIVE EXAMPLES

We conclude by demonstrating the utility of the scheme presented in this paper. Two examples in which this procedure was validated using the experimental data are presented in Figures 10 and 11. In Figure 10, 10% kaolin in a 150 mm flume at a slope of  $5^\circ$  is shown. Figure 11 depicts 1,5% CMC in a 300 mm flume at a  $1^\circ$  slope.

These examples are presented to show that the flow for the materials tested can be predicted reasonably well over a range of flow conditions.

## CONCLUSIONS

This work has shown that it is possible to plot all the data from the flume tests on the standard Moody diagram using the Reynolds number, as suggested by Haldenwang et al (2002). Unlike the case of water flowing in open channels, where mainly turbulent flow occurs, when the fluid becomes more viscous and non-Newtonian, it is much more probable that laminar flow will be encountered.

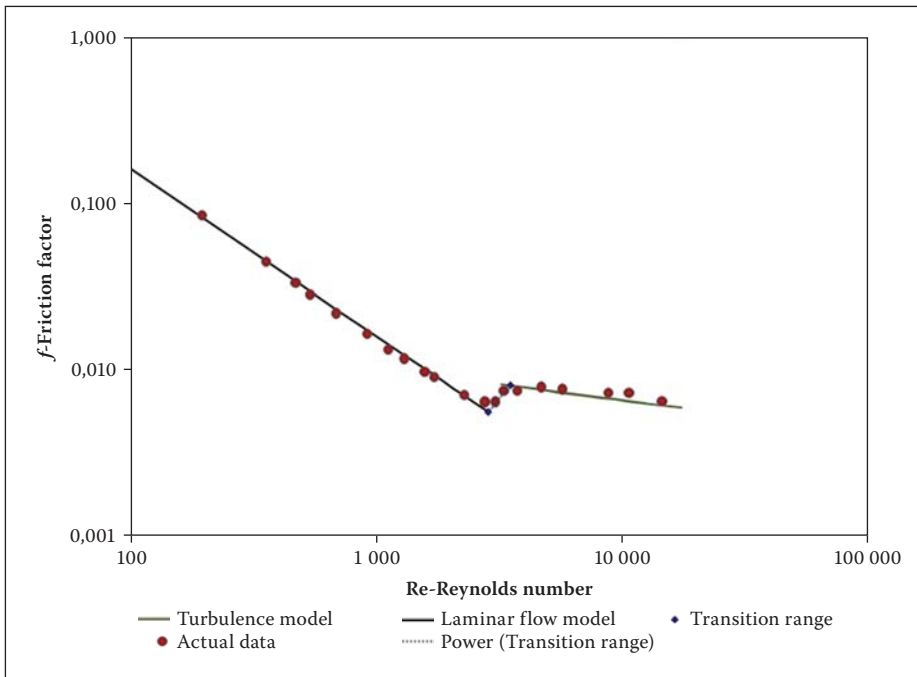


**Figure 11** Moody diagram of 1,5% CMC in 300 mm flume with 1° slope

Therefore it is important to determine the flow regime for a given set of conditions.

While the analysis of the laminar flow regime hinges on sound physical considerations, the treatment of the transitional and turbulent flow regimes is of necessity empirical in nature. The scheme developed here has been validated with experimental data obtained with a range of non-Newtonian fluids representing three rheologically different kinds of fluid. From the tests conducted it is evident that the model can adequately predict the flow of these complex fluids in an open channel. Moreover, to the best of our knowledge, it represents the first attempt at predicting the transitional Reynolds number denoting the end of laminar flow and the onset of fully turbulent flow conditions. It is hoped that future studies in this field will corroborate this approach and/or highlight any weaknesses. On the other hand, it is likely that ongoing experimental studies of velocity profiles, together with computational fluid dynamics (CFD) modelling, will provide fundamental insights into the underlying physical processes. This will, in turn, lead to improved design protocols for non-Newtonian fluids in open channels.

## NOTATION

$B$	classical roughness function	
$C$	ordinate-intercept	
$D$	pipe diameter	m
$D_e$	equivalent diameter	m
$D_h$	hydraulic diameter	m
$d_{85}$	diameter of 85th percentile of particles passing	m

$f$	Fanning friction factor	
$Fr$	Froude number	
$g$	gravitational acceleration	m/s <sup>2</sup>
$H$	height of fluid in flume	m
$K$	fluid consistency index	Pa.s <sup>n</sup>
$L$	length between pressure tappings	m
$L_c$	characteristic length taken as $D$ for pipe flow or $4R_h$ for open channel flow	m
$M$	gradient	
$n$	flow behaviour index	
$n'$	apparent flow behaviour index	
$\Delta p$	pressure drop	Pa
$Re$	Reynolds number	
$Re_c$	critical Reynolds number at onset of transition	
$Re_{c(turb)}$	critical Reynolds number at onset of "full turbulence"	
$R_h$	hydraulic radius	m
$V$	average velocity	m/s
$V_{turb}$	turbulent velocity	m/s
$V_*$	shear velocity	m/s
$w$	flume width	m
$\alpha$	angle of flume from the horizontal	degrees
$\mu$	dynamic viscosity	Pa.s
$\mu_w$	dynamic viscosity of water	Pa.s
$\mu/\dot{\gamma}(100s^{-1})$	apparent viscosity at a shear rate of 100 s <sup>-1</sup>	Pa.s
$\mu/\dot{\gamma}(500s^{-1})$	apparent viscosity at a shear rate of 500 s <sup>-1</sup>	Pa.s
$\dot{\gamma}$	shear rate	s <sup>-1</sup>

$\dot{\gamma}_w$	true shear rate at wall	s <sup>-1</sup>
$\dot{\gamma}_{wn}$	nominal shear rate at wall	s <sup>-1</sup>
$\rho$	density	kg/m <sup>3</sup>
$\tau$	shear stress	Pa
$\tau_w$	wall shear stress	Pa
$\tau_y$	yield stress	Pa
$\chi$	Von Karman constant	

## REFERENCES

- Astarita, G, Marrucci, G & Palumba, G 1964. Non-Newtonian flow along inclined plane surfaces. *Industrial & Engineering Chemistry Fundamentals*, 3(4): 333–339.
- Balmforth, N, Burbridge, A & Craster, R 2000. Viscoplastic models of isothermal lava domes. *Journal of Fluid Mechanics*, 403: 37–65.
- Balmforth, N, Craster, R, Rust, A & Sassi, R 2007. Viscoplastic flow over an inclined surface. *Journal of Non-Newtonian Fluid Mechanics*, 142: 219–243.
- Coussot, P 1994. Steady laminar flow of concentrated mud suspensions in open channels. *Journal of Hydraulic Research*, 32: 535–558.
- Coussot, P 1997. *Mudflow Rheology and Dynamics*. Rotterdam: Balkema.
- Chadwick, A & Morfett, J 1999. *Hydraulics in Civil and Environmental Engineering*. London: E & FN Spon.
- Chanson, H 1999. *The Hydraulics of Open Channel Flow*. London: Arnold.
- Chhabra, R P & Richardson, J F 2008. *Non-Newtonian Flow in the Process Industry*. Oxford: Butterworth-Heinemann.
- Chow, V T 1959. *Open Channel Hydraulics*. New York: McGraw-Hill.
- De Kee, D, Chhabra, R P, Powley, M B & Roy, S 1990. Flow of viscoplastic fluids on an inclined plane: evaluation of yield stress. *Chemical Engineering Communications*, 96: 229–239.
- Douglas, J F, Gasiorek, J M & Swaffield, J A 1985. *Fluid Mechanics*. Essex, UK: Longman Scientific and Technical.
- Govier, G W & Aziz, K 1977. *The Flow of Complex Mixtures in Pipes*. Florida, US: Van Nostrand Reinhold.
- Haldenwang, R 2003. Flow of non-Newtonian fluids in open channels. Unpublished Doctor Technologiae thesis. Cape Town: Cape Technikon.
- Haldenwang, R, Slatter, P T & Chhabra, R P 2002. Laminar and transitional flow in open channels for non-Newtonian fluids. *Proceedings, Hydrotransport 15: 15th International Conference on the Hydraulic Transport of Solids in Pipes*, Banff, Canada, 755–768.
- Huang, X & Garcia, M H 1998. A Herschel-Bulkley model for mud flow down a slope. *Journal of Fluid Mechanics*, 374: 305–333.
- Kozicki, W & Tiu, C 1967. Non-Newtonian flow through open channels. *Canadian Journal of Chemical Engineering*, 45: 127–134.



- Manning, R 1890. On the flow of water in open channels and pipes. *Transactions of the Institution of Civil Engineering Ireland*, 20: 161–207.
- Mei, C C & Yuhi M 2001. Slow flow of a Bingham fluid in a shallow channel of finite width. *Journal of Fluid Mechanics*, 431: 135–159.
- Naik, B 1983. Mechanics of mudflow treated as the flow of a Bingham fluid. PhD thesis, USA: Washington State University.
- Paslay, P R & Slibar, A 1958. Flow of an incompressible visco-plastic layer on an inclined plane. *Journal of Rheology*, 2: 255–262
- Sanders, R S, Schaan, J, Gillies, R G, McKibben, M J, Sun, R & Shook, C A 2002. Solids transport in laminar open-channel flow of non-Newtonian slurries *Proceedings, Hydrotransport 15: 15th International Conference on the Hydraulic Transport of Solids in Pipes*, Banff, Canada, 597–611.
- Slatter, P T 1996. Modelling the turbulent flow of non-Newtonian slurries. *R&D Journal (South African Institution of Mechanical Engineering)*, 12: 68–80.
- Slatter, P T 1999. The role of rheology in the pipelining of mineral slurries. *Mineral Processing and Extractive Metallurgy Review*, 20: 281–300.
- Slatter, P T & Lazarus, J H 1993. Critical flow in slurry pipelines. *Proceedings, Hydrotransport-12: 12th International Conference on Slurry Handling and Pipeline Transport*, Brugge, Belgium, 639–654.
- Sylvester, N D, Tyler, J S & Skelland, A H P 1973. Non-Newtonian thin films: theory and experiments *Canadian Journal of Chemical Engineering*, 51: 418–429.
- Taylor, A J & Wilson, S D R 1997. Conduit flow of an incompressible, yield-stress fluid. *Journal of Rheology*, 41: 93–102.
- Therien, N, Coupal, B & Corneille, J L 1970. Verification experimentale de l'épaisseur du film pour des liquides non-Newtonien's écoulant par gravité sur un plan incliné. *Canadian Journal of Chemical Engineering*, 48: 17–20.
- Uhlherr, P H T, Park, K H, Tiu, C & Andrews, J R G 1984. Yield stress from fluid behaviour on an inclined plane. *Proceedings, IXth International Congress on Rheology*, Acapulco, Mexico, 183–188.
- Wilson, K C 1991. Slurry transport in flumes (Chapter 8). In: Brown, N P & Heywood, N I (Eds), *Slurry Handling: Design of Solid-Liquid Systems*, London: Elsevier Applied Science, 167–180.
- Wilson, S D R & Taylor, S J 1996. The channel entry problem for a yield stress fluid. *Journal of Non-Newtonian Fluid Mechanics*, 165: 165–176.